JOURNAL OF CATALYSIS 33, 392–401 (1974)

The Formation and Reactivity of Oxygen as O_2^- on a Supported Silver Surface

R. B. CLARKSON AND A. C. CIRILLO, JR.

Department of Chemistry and Laboratory for Surface Studies, University of Wisconsin-Milwaukee, Milwaukee, Wisconsin 53201

Received November 6, 1973

The formation and reactivity of O_2^- on a Vycor quartz supported silver catalyst has been investigated by electron paramagnetic resonance spectroscopy (EPR). The silver catalyst was characterized by transmission electron microscopy and electron diffraction, and revealed that the silver is in the form of small particles with a mean diameter of 47 Å. Surface aging under OAOR (outgassing–adsorption–outgassing–reduction) cycling produced a decrease in the activity of the silver surface with respect to O_2^- formation which coincided with the appearance of electron diffraction patterns characteristic of Ag_2O. Studies of the kinetics of O_2^- formation by EPR in the temperature range 298–333 K yielded a value of E_a (desorption) of 14.8 kcal/mol for O_2^-, as analyzed by a simple mechanism for superoxide formation. Isotherms for total O_2 adsorbed and O_2^- formed showed a saturation uptake of O_2 at 298 K equivalent to $\theta = 0.44$, and a $[O_2^-]/[O_2]$ ratio of 0.02% at that temperature. Finally, the kinetics of the reactivity of O_2^- with CO were investigated, and suggest that O_2^- is the reactive species in the silver catalyzed oxidation of CO to CO_2, or is the direct parent of the reactive species.

INTRODUCTION

The rate and nature of the adsorption of oxygen on silver surfaces has been the subject of numerous investigations. Chemisorption data using a variety of techniques have suggested that adsorbed oxygen may exist on silver in a variety of forms: O (atom), O^-, O_2, O_2^-, O_2^{2-}. Czanderna, using an ultramicrobalance technique, suggested that three distinct adsorbed states corresponding to activation energies of adsorption of 3, 8, and 22 kcal/mol were present on pretreated silver surfaces (*1*, *2*). Kilty, Roland and Sachtler (*3*) have noted the probable role of O_2^- in the silver catalyzed oxidation of ethylene to ethylene oxide. Finally, FEM studies by Czanderna, Frank and Schmidt (*4*) have suggested that an undissociated form of oxygen exists on silver tips that have been exposed to molecular oxygen at 10^{-3} Torr (1 Torr = 133.3 N m^{-2}) for 1 min at temperatures from 50 to 200°C.

Interest in oxygen adsorbed on silver as O_2^- is derived from a variety of sources, including questions as to the species' role in the catalytic oxidation of ethylene (*3*) and CO (*5*), and the overall mechanism of oxygen adsorption on silver. Recently, we published data confirming the existence of the peroxide radical ion using an EPR technique (*6*). In this investigation, we use the paramagnetic resonance of O_2 and O_2^- to follow the kinetics of O_2^- formation on Vycor quartz supported silver surfaces at a variety of temperatures to obtain information on the activation energies of desorption of the peroxide species as well as to gain insights into silver surface modifications occurring under a Czanderna type OAOR (outgassing–adsorption–outgassing–reduction) cycling of the sample, which affects the ability of the surface to form O_2^-. Equilibrium experiments also are reported to compare total O_2 uptake with the surface

concentration of O_2^-. Finally, the reaction kinetics of O_2^- with CO have been followed and the results were analyzed according to a simple mechanism.

Methods

Silver surfaces were formed on Vycor glass supports by the incipient wetness technique. Porous Vycor quartz glass rods (Corning, lot No. 7930) were pretreated with concentrated HNO_3 and rinsed thoroughly with distilled water. The rods were evacuated at 550°C, and then treated for 24 hr with O_2, evacuated, and then treated with H_2 for 12 hr to remove contaminants. Final evacuation to a pressure of 3×10^{-7} Torr yielded support blanks that gave no EPR signals at room temperature and at liquid nitrogen temperatures, even after 20 min of intense uv irradiation. Further, the Vycor rods were inert to the introduction of O_2, forming no radical species on the surface. The glass exhibited a surface area of 132.1 m^2/g as determined at liquid nitrogen temperatures by a BET plot of O_2 adsorption.

The clean Vycor rods then were immersed in a 0.098 M aqueous solution of $AgNO_3$ (Mallinckrodt, Analytical Reagent). After 24 hr, the rods were dehydrated by evacuation and the Ag^+ was reduced to the metal under 760 Torr of H_2 at 130°C. Then the excess H_2 and reduction products were removed by evacuation to 3×10^{-7} Torr at the reduction temperature. Silver surfaces prepared in this fashion showed no EPR signals at room temperature and liquid nitrogen temperature and had a glossy black appearance when viewed with reflected light. The loading of such supported silver samples was 0.3% by weight.

All gases used in the experiments were experimental grade, twice purified through liquid nitrogen cold traps. In the case of O_2, the vapor pressure of liquid O_2, twice distilled in vacuum, was used as the source of gaseous oxygen.

EPR spectra were obtained on a Varian E-3 spectrometer equipped with the variable temperature accessory. Liquid helium temperature spectra were obtained using a Magnion X-band spectrometer (9.5 in.). Gaseous oxygen pressure changes occurring during a run were monitored by observing the change in EPR line width of the $k = 1$, $J = 1$, $\Delta m = 0 \rightarrow 1$ line of gaseous oxygen observed at 6,416 G with a microwave frequency of 9.410 GHz. O_2^- line intensity changes were determined by tracing the first derivative signals and weighing the area under the curve. Absolute spin concentrations were calculated using a Varian weak pitch standard (10^{13} spins/c of length).

For kinetic studies, it was convenient to keep the gaseous O_2 pressure constant while monitoring the change in O_2^- signal intensity. For this purpose, the ballast doser illustrated in Fig. 1 was used. It permitted temperature equilibration of the assembly at the spectrometer and use of the pressure broadened gaseous O_2 EPR line was an internal standard on oxygen pressure throughout a run. In dosing experiments aimed at studying equilibrium O_2^- concentration as a function of temperature and total O_2 uptake, the total amount of oxygen adsorbed was measured using the technique of Clarkson and Turkevich (7).

Silver particle size and surface structure was determined using a Hitachi HU-11B electron microscope fitted with a high resolution electron diffraction stage. 75 kV electrons were used in the diffraction work; evaporated gold films were used as calibration standards.

OAOR cycling was used on some silver

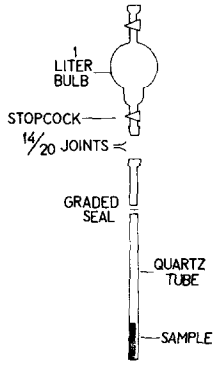

FIG. 1. Doser assembly used in EPR studies of formation and reactivity of O_2^- on silver.

samples to "age" the surface to a reproducible activity for the formation of O_2^-. In such cases, the OAOR cycle consisted of the following:

1. Outgas the sample at 160°C to 4×10^{-7} Torr for 6 hr;
2. Adsorb oxygen under experimental conditions;
3. Outgas sample as in Step 1; and
4. Reduce surface under 400 Torr of CO at 160°C for 24 hr.

Such a cycle generated a sample again free

FIG. 2. Transmission electron micrograph of silver particles in the pore structure of Vycor quartz; ×125,000.

of EPR signals (spectrometer sensitivity of $S/N = 200:1$ for 4×10^{13} spins). Omission of Step 4 left a small O_2^- signal, as discussed below.

Results

A. Sample Characterization

Figure 2 shows an electron micrograph of a chip of 3 mm diameter porous Vycor quartz rod impregnated with silver. Silver particles range in size from 30 to 100 Å and can be seen to be separated, without evidence of agglomeration. Undoubtedly the pore structure of the glass is critical in maintaining silver particle separation. Samples of silver supported in this fashion showed a surface area of about 121 m^2/g, calculated geometrically by assuming spherical particles of radius r, and integrating over the distribution of r exhibited in the micrographs. The distribution gives a mean value of $2r$ of 47 Å.

When freshly prepared, silver samples were amorphous, showing no clear electron diffraction pattern. After heating in vacuum at 350°C for 24 hr, sintering produced microcrystallinity, as evidenced by clearly measurable but diffuse diffraction ring patterns characteristic of metallic silver. After 30 OAOR cycles (described previously), very clear diffraction patterns were observed. Based on intensity and line spacing measurements of the first nine diffraction rings, this pattern fits well the pattern expected for Ag_2O. We therefore postulate that in the "aging" of a silver surface under a controlled OAOR cycling scheme, the changes in surface activity to the formation of O_2^- are due to the building up of a stable Ag_2O layer on the surface of silver particles, and that achievement of this stable surface oxide layer constitutes the principal condition for a "reproducible surface" as defined by Czanderna for silver (*1*, *2*). As we shall see, this "aging" process effects both kinetic and equilibrium phenomena associated with O_2 adsorption. It should be noted here that in work described below, effects observed on silver surfaces coated with silver(I) oxide could not be duplicated using Ag_2O powder alone.

B. EPR Spectral Data

A detailed account of the theory of the g-tensor for O_2^-, together with a comparison of our measured principal g-values with others reported in the literature has already been published (*6*). Figure 3 illustrates a typical X-band EPR spectrum of the superoxide at room temperature. The integrated intensity of this signal is proportional to the surface O_2^- concentration. No other paramagnetic resonance signals were observed in any of our samples (other than those arising from the paramagnetic gaseous oxygen itself) over a temperature range from 333 to 1.5 K. At lower temperatures, very little line narrowing was observed, leading us to believe that the O_2^- signal is inhomogeneously broadened due to adsorption site irregularities. The O_2^- signal appeared after the introduction of oxygen into the sample at all temperatures from 77 K up (temperatures below 77 K were not accessible to our doser arrangement, so O_2 was introduced at room temperature and the tubes were sealed for liquid helium temperature spectra).

The principal g-values measured for our sample, together with the crystal field splitting parameters arising from a component of electric field perpendicular to the interatomic axis of O_2^-, are very close to those reported by Lunsford and Jayne for O_2^- on ZnO (*8*). Table 1 compares our results with those of Lunsford and Jayne (*8*) for O_2^- on ZnO and of Miller and Haneman (*14*) for O_2^- on clean AlSb. This comparison extends our HEED studies and suggests that O_2^- adsorbs, not on a bare Ag metal surface, but rather on a surface that has become oxidized even if OAOR cycling has not been imposed on the sample. This

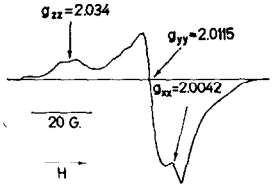

FIG. 3. X-Band EPR spectrum at room temperature of O_2^-, the paramagnetic species formed when oxygen adsorbs on Ag.

TABLE 1
COMPARISON OF EPR PARAMETERS OBTAINED FOR O_2^- ON SEVERAL SUBSTRATES

Material	G_{xx}	G_{yy}	G_{zz}	λ/δ	λ/Δ
O_2^- on silver	2.0042	2.0115	2.034	0.016	0.0037
O_2^- on ZnO[a]	2.0020	2.0082	2.051	0.017	0.0032
O_2^- on AlSb[b] (freshly cleaved)	2.002	2.005	2.041	0.019	0.0015

[a] Ref. (*8*).
[b] Ref. (*14*).

we conclude from the following argument: the surface potential of clean and oxided (or contaminated) silver metal has been shown to be drastically different by such techniques as LEED (*9–11*), Auger spectroscopy (*11–12*), contact potential studies (*11*), and FEM data (*4*, *13*). Such changes in surface potential would strongly alter the electric field experienced by an O_2^- molecule adsorbed on silver, and hence alter the perturbation of molecular energy levels in the superoxide ion that account for the g-values observed in our EPR studies. The g-values and associated crystal field splittings measured by us for O_2^- on both OAOR cycled and fresh silver surfaces show small differences, and are, in fact, so close to those reported for O_2^- on ZnO that we conclude that under all experimental conditions reported in this paper, O_2^- is adsorbed, not on bare Ag, but on a silver oxide, though not necessarily a stoichiometric oxide. For comparison to a much cleaner surface, note the value for λ/Δ for O_2^- on AlSb in Table 1. The much larger value of Δ gives evidence that in that system the O_2^- adsorbed on a site giving rise to a greater perturbation of the σ_{2p}–π_y^* orbitals. The freshly cleaved nature of Miller and Haneman's (*14*) surface may well account for this stronger field perturbation.

Finally, it should be mentioned that pumping for days on a Ag–O_2^- sample at a pressure $<2 \times 10^{-7}$ Torr and at a temperature of 160°C failed to remove the O_2^- signal, although its intensity could be reduced by about 85%. Only chemical reduction could completely remove the resonance line. CO was chosen as the reducing gas when this was necessary, since future experiments plan to investigate the role of O_2^- in the silver catalyzed oxidation of CO.

C. Kinetics of O_2^- Formation

The time rate of change of the O_2^- EPR signal intensity was monitored to obtain data on the kinetics of the formation of the superoxide on fresh and OAOR cycled silver surfaces. Equating integrated EPR signal intensity with spin concentration by the weighing of signal tracings has proven to be an accurate analytical technique, with an error of $\sim \pm 5\%$ (*15*). We therefore assert:

$$\frac{dI}{dt} \propto \frac{d[O_2^-]}{dt}, \tag{1}$$

where I is the integrated intensity of the resonance line of O_2^-.

Using the doser arrangement described under "Methods" above, kinetic studies were made at the following temperatures: 313, 318, 323, 328, and 333 K. In each case, the oxygen overpressure was held constant at 0.5 Torr as measured by the pressure-broadened $J = 1$, $K = 1$, $\Delta m = 0 \rightarrow 1$ line of gaseous oxygen. A plot of I vs time for an OAOR cycled sample at 333 K is shown in Fig. 4, and is typical of data obtained at other temperatures. Data could not be

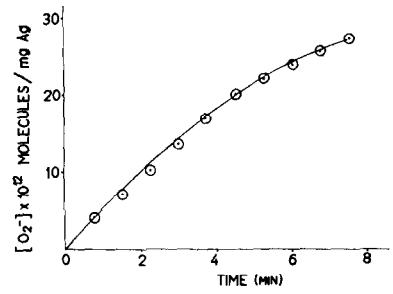

FIG. 4. The variation of integrated EPR line intensity of O_2^- (I) with time at 333 K, 0.5 Torr oxygen.

taken during the first 30 s after dosing, because of the spectrometer relaxation time. Since, as we shall see, the rate of O_2^- formation and the equilibrium O_2^- concentration achieved at any temperature is a sensitive function of surface pretreatment, all comparisons of kinetic data observed at different temperatures were made on single samples that had been "aged" to a constant surface activity. Many kinetic mechanisms were tried on the data obtained from EPR studies.

The highly exponential character of all I vs time curves led us to postulate, as a simple mechanism for O_2^- formation, the following:

$$\begin{aligned} O_2\,(g) &\xrightarrow{k_1} O_2^-, \\ O_2^- &\xrightarrow{k_{-1}} O_2\,(g). \end{aligned} \tag{2}$$

Thus,

$$\frac{d[O_2^-]}{dt} = k_1[O_2] - k_{-1}[O_2^-]. \tag{3}$$

Now in our experimental arrangement of constant O_2 pressure, the integration of Eq. (3) yields

$$\ln\left(\frac{k_1[O_2] - k_{-1}[O_2^-]}{k_1[O_2]}\right) = -k_{-1}t. \tag{4}$$

At equilibrium, $k_1[O_2] = k_{-1}[O_2^-]$, and therefore,

$$\frac{[O_2^-]}{[O_2]} = K = \frac{k_1}{k_{-1}},$$

where K is the equilibrium constant for the reaction. So, Eq. (4) becomes

$$\ln\left(\frac{K[O_2] - [O_2^-]}{K[O_2]}\right) = -k_{-1}t. \tag{5}$$

But $K[O_2] = [O_2^-]_{\text{equilib}}$, and if the integrated EPR signal intensity of O_2^-, $I = \text{const}[O_2^-]$, then Eq. (5) becomes

$$\ln\left(\frac{I_0 - I}{I_0}\right) = -k_{-1}t, \tag{6}$$

where I_0 is the equilibrium O_2^- signal intensity at any temperature. Thus, a plot of $\ln[(I_0 - I)/I_0]$ vs t should yield a straight line of slope, $-k_{-1}$. Such a plot is shown in Fig. 5, for the 333 K run, and illustrates the high degree of correlation which all our rate data exhibited when reduced according to Eq. (6). Table 2 lists the variation of k_{-1} with temperature, together with the coefficient of correlation obtained from a computer least squares straight line fit of the data for each run.

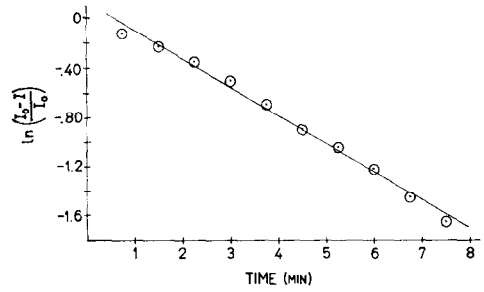

FIG. 5. $\ln[(I_0 - I)/I_0]$ vs time, illustrating the correlation of data with that predicted in Eq. (6).

From Eq. (6) we note that a temperature dependence exists for I_0 as well as for k_{-1}. However, the presence of I_0 in numerator and denominator of Eq. (6) insures that changes in equilibrium O_2^- concentration with temperature will be normalized, so comparison of k_{-1} values at different temperatures can be made.

Accordingly, we made an Arrhenius plot of $\ln k_{-1}$ vs $1/T$ to obtain the activation energy for desorption of O_2^- from our data. Such a plot is shown in Fig. 6. Difficulties in preparing samples for each temperature run which have identical surface properties undoubtedly account for some of the scatter which is observed. Yet despite these experimental difficulties, the activation energy for desorption of O_2^- from silver calculated from the slope of the Arrhenius plot of Fig. 6, where each point represents an average of

TABLE 2
VARIATION OF k_{-1} WITH TEMPERATURE FROM BEST STRAIGHT LINE PLOTS

T (K)	k_{-1} (min^{-1})	Coefficient of correlation of best straight line
313	0.0470	0.804
318	0.1335	0.999
323	0.179	0.994
328	0.174	0.942
333	0.1230	0.996

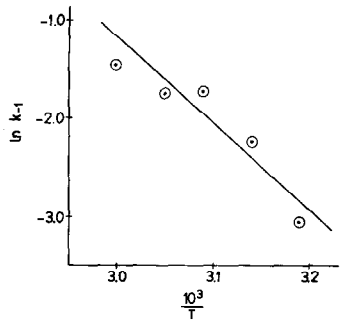

FIG. 6. Arrhenius plot of ln k_{-1} vs $1/T$. The slope of the line is $-7.4 = -E_a/(R \times 1000)$.

k_{-1} for several samples, is 14.8 kcal/mol (±10%), in agreement with the value of E_a (desorption) = 15.9 kcal/mol obtained by Czanderna, Chan and Biegen (*16*) for the activation energy of desorption of oxygen from silver in our temperature region.

D. Equilibrium Adsorption

The total oxygen uptake was compared to surface O_2^- concentration in fresh and OAOR cycled silver samples. Also, the variation of equilibrium O_2^- surface concentration with temperature was examined.

Using the dosing EPR technique discussed by Clarkson and Turkevich (*7*), we followed the total O_2 adsorption on fresh silver samples at 298 K, at the same time monitoring the increase in O_2^- concentration. To insure equilibration, 24 hr was allowed between doses. Figure 7 illustrates these results. At 298 K, both the total adsorption of oxygen and the formation of O_2^- show a progressive saturation. The total O_2 uptake saturates at about 0.6 Torr at 298 K with a total uptake average of 3.7×10^{17} molecules/mg Ag. The saturation value of O_2^- under the same conditions (and measured on the same samples as total O_2 uptake) was 6.9×10^{13} O_2^-/mg Ag. Recalling that our samples had a geometric surface area of 121 m^2/g and that the average mass of silver in samples used in these experiments was 1.8 mg, we calculate a saturation coverage of 3.1×10^{18} molecules/m^2 for total O_2 at 298 K. Taking Kilty, Rol and Sachtler's value (*3*) of an oxygen monolayer ($\theta = 1$) on silver to be 7×10^{18} molecules/m^2, we find a saturation coverage

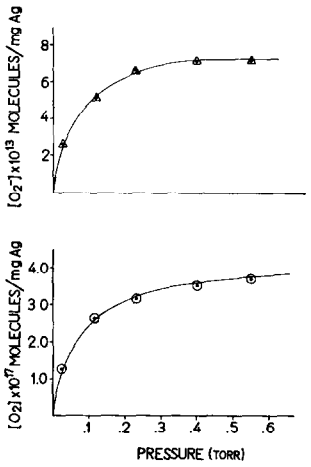

FIG. 7. O_2 and O_2^- concentration on Ag surface as a function of oxygen pressure at 298 K.

of $\theta = 0.44$. As Czanderna amply illustrates from the literature (*17*), this value is comparable to the saturation coverage measured by others for oxygen on silver at this temperature and pressure.

Taking the ratio of $[O_2^-]_{ads}$/total $O_{2\ ads}$ at saturation, we find that about 0.02% of all oxygen adsorbed is in the form O_2^-. Several years ago, Kummer (*18*) used the rate of *ortho–para* hydrogen conversion to estimate the fraction of adsorbed O_2 on silver which was paramagnetic. On *evacuated* Ag samples, he found *ortho–para* conversion rates suggestive of a paramagnetic: chemisorbed O_2 ratio of ~5%. While we did not pump our samples to measure the total oxygen removed, we did follow the O_2^- signal intensity during evacuation. We could not reduce the signal by more than 85% under prolonged pumping at 150°C in the low 10^{-7} Torr range. Therefore, we feel our low ratio of $[O_2^-]_{ads}$/total $O_{2\ ads}$ supports Kummer's earlier observation, and would further suggest that over 90% of the oxygen adsorbed on our sample is reversibly adsorbed (i.e., is removable by pumping), consistent with Czanderna's findings (*1*).

Finally, we plot the equilibrium O_2^- signal intensity as a function of temperature at constant O_2 pressure to see ΔH_{ads} vary as T. The O_2 overpressure is held constant (isobar) at 0.5 Torr and a straight line plot should result when the log of the

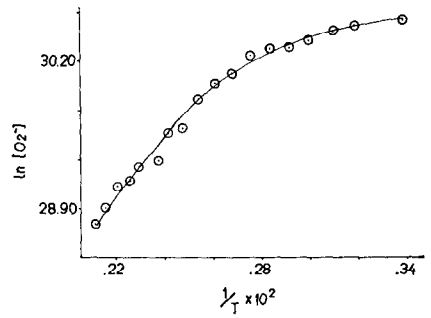

FIG. 8. Isobar (0.5 Torr) of the log e of equilibrium O_2^- surface concentration (ln I_{equi}) vs $1/T$.

equilibrium line intensity at any temperature (ln I_{equi}) is plotted against $1/T$, since

$$I_{equi} = C\sigma = Ck_2 \frac{e^{\Delta H_{ads}/RT}}{(T)^{1/2}},$$

where σ is the amount of gas adsorbed/unit area and C and k_2 are constants. Such a plot is shown in Fig. 8. The nonlinearity of the plot indicates ΔH is a function of T and probably of θ. From Fig. 8, one can calculate that ΔH_{ads} for O_2^- varies from -1.3 kcal/mol at 295 K to -7.5 kcal/mol at 473 K, a familiar range of H_{ads} for the species postulated to be the molecular ion.

E. Variation of Rate of Adsorption and Equilibrium O_2^- Concentration with OAOR Cycling

Figure 9 illustrates the variation of the rate of formation and the equilibrium concentration of O_2^- as a function of OAOR cycle. One observes an initial decrease of both parameters, with an inflection point at the 7th cycle, followed by recovery of the catalyst activity, peaking at the 9–10th cycle, but continuing to change out past 30 cycles. It should be noted that the very large number of OAOR cycles needed to produce a "reproducible surface" is a function of catalyst support; 15 cycles seem sufficient to obtain reproducibility when silver is supported on alumina, while Vycor supports require over 30 cycles to achieve the same state.

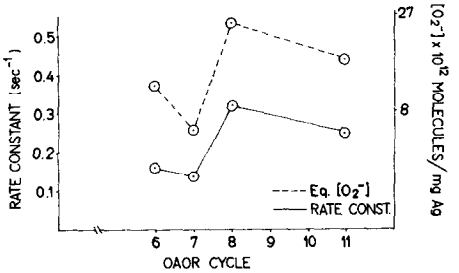

FIG. 9. Variation of rate of formation of O_2^- and equilibrium O_2^- concentration as a function of sample aging (OAOR cycle number).

The ability of silver catalysts to regain activity after initial decreases in use has been noted by others. In our investigation, the reversal of activity loss as a function of OAOR cycle number corresponded to a dramatic change in the HEED pattern of the surface, the diffraction rings going from diffuse to sharp between the 7th and 10th cycles. This leads us to speculate that, upon formation of stoichiometric Ag_2O with regular crystal structure (as indicated by sharp HEED ring pattern), electron transport from the Ag metal, through the surface oxide, to the adsorbed oxygen is rendered easier, perhaps because of the change in the oxide layer from a relatively amorphous semiconductor to a well-defined crystalline surface layer semiconductor. An investigation of surface oxide rearrangement and its relationship to the ability of the Ag metal to form O_2^- is currently being undertaken in this laboratory.

F. Reactivity of O_2^- with CO

Using the doser (constant pressure) arrangement described under "Methods" above, we followed the decrease of the O_2^- EPR signal intensity when CO was introduced to silver samples with preadsorbed oxygen present. Adopting the mechanism for the $CO + \frac{1}{2}O_2 \xrightarrow{Ag} CO_2$ reaction proposed by Keulks and Chang (*5*), and defining the extent of reaction by X, we write, for the instantaneous concentration of CO, CO_2 and O_2^-:

$$n_{CO} = n_{CO}^0 - 2X$$
$$n_{CO_2} = n_{CO_2}^0 - 2X$$
$$n_{O_2^-} = n_{O_2^-}^0 - X,$$

where n_i = instantaneous concentration and n_i^0 = concentration of i at time zero.

Working in a regime of limiting reactants (i.e., CO or O_2^-) we can define a parameter

$$f = X/X_{max},$$

where X_{max} is defined as the extent of the reaction when the limiting reactant is completely consumed. Then for the case when CO is the limiting reaction, one can write:

$$P_{CO}{}^0 f + P_{CO}{}^0 \ln(1 - f) = -kt, \quad (7)$$

and when O_2 is the limiting reactant,

$$2P_{O_2}{}^0 f + P_{CO}{}^0 \ln[1 - (2P_{O_2}{}^0/P_{CO}{}^0)f] = -kt. \quad (8)$$

Equations (7) and (8) may be related to the time rate of change of the O_2^- EPR signal by stating:

$$f = X/X_{max} = \text{const}[(I^0 - I)/I^0]. \quad (9)$$

One then plots I vs time and compares the curves thus obtained to those predicted by Eqs. (7) and (8), using Eq. (9) to relate I to f. Both O_2 and CO limited reactions were run and are illustrated in Fig. 10a and b. The excellent agreement between the predicted rate laws and experiment supports the notion that either O_2^- is the reactive oxygen species in the silver catalyzed oxidation of CO or that it is in rapid equilibrium with the reactive species.

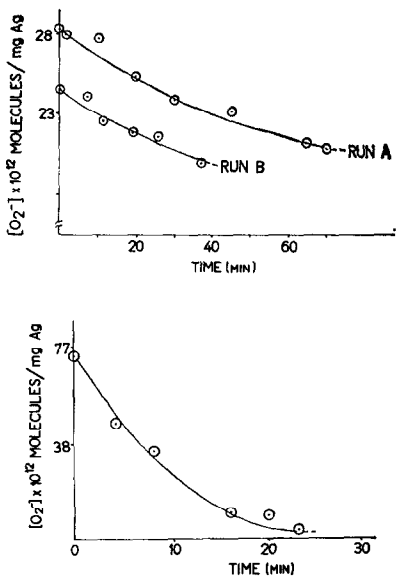

FIG. 10a. (top) Two plots showing O_2 limited reaction of O_2^- with CO at 298 K. Curves A and B differ in starting concentration of O_2^-; they are fit by the same rate constant. (—) Theoretical curve predicted by Eq. (8). (b) (bottom) Plot of CO limited reaction of O_2^- with CO at 298 K. (—) Theoretical curve predicted by Eq. (7).

DISCUSSION

Combining EPR and electron diffraction data for O_2^- adsorbed on supported silver leads us to a picture of the silver surface that suggests the presence of a surface oxide layer, even after the first OAOR cycle. Electron transfer from the metal to adsorbed oxygen is rendered more difficult by this surface layer, and hence we see a decrease in the activity of the catalyst to O_2^- formation as the OAOR cycling proceeds. Achievement of a stoichiometric Ag_2O layer, signaled by the appearance of sharp electron diffraction rings, restores some of the catalytic activity, probably by establishing a well-defined electronic band structure in the Ag_2O, which assumes the properties of a semiconductor in facilitating electron transport from the substrate silver to the oxide surface.

Transmission electron microscopy gives us the opportunity to assess the geometric form of silver in the pores of the Vycor quartz support. Corning Vycor (No. 7930) is known to have very uniform pores of a diameter ~70 Å, so our silver particles, with a mean diameter of 47 Å do not clog pores, as can be demonstrated by the fact that a nitrogen BET surface area measurement of silver loaded Vycor does not change the free glass surface area. The equilibrium uptake of oxygen at 298 K combined with a calculated surface area of silver gives a commonly observed value of $\theta = 0.44$ at 0.5 Torr of oxygen. Further, it is not inconsistent with one model of oxygen adsorption on silver to calculate that only 0.02% of all adsorbed oxygen is O_2^- at equilibrium conditions, and still have O_2^- play an important role in oxidation catalysis.

This model suggests that at low temperatures, ~300 K, where dissociative adsorption is not an important process—at least as assessed by $^{16}O_2$-$^{18}O_2$ isotopic scrambling experiments (*19*)—the vast majority of oxygen chemisorbs as molecular oxygen,

O_2, which is rendered nonparamagnetic by anisotropic surface electric fields [see Ref. (*14*)]. O_2^- may form only on high index planes of the surface oxide, or on surface defects; that there is a considerable heterogeneity to the O_2^- adsorption site is evidenced by the inhomogeneously broadened EPR signal derived from the superoxide. The excellent agreement between theoretical rate laws derived for CO oxidation in this system and the experimentally determined time rate of change of $[O_2^-]$ lends further support to the contention that O_2^- is the reactive oxygen species at these low temperatures, or is the parent of an extremely short-lived monatomic form of oxygen, unseen by EPR, which actually participates in the CO oxidation.

Finally, agreement between the activation energy for desorption of O_2^- calculated from our EPR kinetic studies with those of Czanderna using ultramicrobalance techniques suggests that we are observing the kinetics of a desorption step whose activation energy is an average energy brought about by a stepwise desorption: O_2^- (ads) $\rightarrow O_2$ (ads) $\rightarrow O_2$ (g). Further studies of adsorption kinetics in the temperature region around 300 K seem essential if one is to answer the many points that remain unresolved in the mechanism of O_2 adsorption on silver.

Acknowledgment

Acknowledgment is made to the Donors of the Petroleum Research Fund, administered by the American Chemical Society, for the support of this research.

References

1. Czanderna, A. W., *J. Phys. Chem.* **68**, 2765 (1964).
2. Czanderna, A. W., *J. Phys. Chem.* **70**, 2120 (1966).
3. Kilty, P. A., Rol, N. C., and Sachtler, W. M. H., *J. Catal.* **28**, 209 (1973).
4. Czanderna, W. A., Frank, O., and Schmidt, W. A., *Surface Sci.* **38**, 129 (1973).
5. Keulks, G. W., and Chang, C. C., *J. Phys. Chem.* **74**, 2590 (1970).
6. Clarkson, R. B., and Cirillo, A., Jr., *J. Vac. Sci. Technol.* **9**, 1073 (1972).
7. Clarkson, R. B., and Turkevich, J., *J. Colloid Interface Sci.* **38**, 165 (1972).
8. Lunsford, J. H., and Jayne, J. P., *J. Chem. Phys.* **44**, 1487 (1966).
9. Müller, K., *Z. Naturforsch.* **20a**, 153 (1965).
10. Mattera, A. M., Goodman, R. M., and Somorjai, G. A., *Surface Sci.* **7**, 26 (1967).
11. Rovida, G., Ferroni, E., Maglietta, M., and Pratesi, F., "Adsorption-Desorption Phenomena," p. 417. Academic Press, New York, 1972.
12. Lassiter, W., *J. Vacuum Sci. Technol.* **9**, 310 (1972).
13. Schmidt, W. A., Frank, O., and Czanderna, A. W., *Phys. Status Solidi* **16**, 127 (1973).
14. Miller, D. J., and Haneman, D., *Phys. Rev.* **3**, 2918 (1971).
15. Poole, C. P., Jr., "Electron Spin Resonance," p. 591. Wiley (Interscience), New York, 1967.
16. Czanderna, A. W., Chen, S. C., and Biegen, J. R., *J. Catal.* **33**, 163 (1974).
17. Czanderna, A. W., *Thin Solid Films* **12**, 521 (1972).
18. Kummer, J. T., *J. Phys. Chem.* **63**, 460 (1959).
19. Keulks, G. W., private communication.